

# Investigation of the Sequence-Dependent dsDNA Mechanical Behavior using Clustered Atomistic-Continuum Method

Chang-An Yuan\*, Cheng-Nan Han\* and Kou-Ning Chiang\*\*

\*Research Assistant, Department of Power Mechanical Engineering, National Tsing Hua University,  
101, Sec. 2, Kuang-Fu Rd., HsinChu Taiwan 300

\*\*Professor, Department of Power Mechanical Engineering, National Tsing Hua University,  
101, Sec. 2, Kuang-Fu Rd., HsinChu Taiwan 300, knchiang@pme.nthu.edu.tw

## ABSTRACT

A novel clustered atomistic-continuum method (CACM) based on the transient finite element theory is proposed herein to simulate the dynamic structural transitions of the double strand DNA (dsDNA) under external loading. Moreover, the meso-mechanics of dsDNA molecules is then studied via the CACM model, including the base-stacking interaction between DNA adjacent nucleotide base pairs, the hydrogen bond of complementary base-pairs and electrostatic interactions along DNA backbones. Additionally, the mechanics of the dsDNA unzip is studied by the verified dsDNA CACM model.

**Keywords:** Single molecule simulation, DNA, Finite element method, Equivalent theory, Meso-mechanics

## 1 INTRODUCTION

The single molecule manipulation technique has been developed for years to measure the basic physical properties of double-stranded DNA (dsDNA) and to discover the interaction between dsDNA and proteins/enzymes [1]. Moreover, the results of the freely-untwisting dsDNA stretching experiment have indicated that a sharp structural transition occurs under roughly 65pN of tension, and that the classical B-form DNA structure dramatically transits to a S-form DNA structure [2-4]. However, the resolution of the single molecule measurement technique currently available restricts the researchers to completely clarify the mechanical behavior of stretching dsDNA as well as the continuous geometrical deformation of the sugar-phosphate chain during stretching. To overcome the resolution limitation of the single molecule manipulation technique, the molecular biology researcher essentially requires an accurate theoretical model to represent the dsDNA mechanical characteristics under specific external loading and boundary condition. However, a feasible numerical model to describe the dsDNA mechanics is difficult to achieve, because the meso-mechanics of single-molecule dsDNA include both quantum mechanics and continuum mechanics. Benham [5] have derived the analytical wormlike rod chain model (WLRC model), and Marko et al. [6] have improved the accuracy of Benham's WLRC model. These WLRC models could predict the DNA mechanical response under low level stretching. However, the WLRC model could not accurately describe the P-form and S-form DNA under high

level stretching force and twisting torque. Zhou et al. [7] have proposed the unique Zhou, Zhang and Ou-Yang model (ZZO model), which considers the bending energy and the base pairs staking energy of dsDNA. The ZZO model could successfully describe the S-type DNA under high level stretching, but it could hardly represent the structural transition from the B-form DNA to the P-form DNA due to its limitation of geometric assumption. Additionally, these theoretical models mentioned above could not provide the dynamic dsDNA structural transition in virtuality. Therefore, a novel clustered atomistic-continuum method based on the transient finite element method with material/geometrical nonlinear properties is applied to illustrate the mechanical behavior of dsDNA under external loading.

The CACM comprises the clustered atomistic method and the atomistic-continuum method. In order to reduce the computational time efficiently, the clustered atomistic method treats the specific clustered atom groups as the clustered elements in the modeling (e.g. the sugar-phosphate backbone of dsDNA). Moreover, the virtual elements describe the interactions between atoms or clustered atomistic groups via the atomistic-continuum method. Therefore, a CACM model of the freely-untwisting dsDNA, which only single strand is fixed at each end, could be then conducted, as indicated in Figure 1 (Fig. 1). Notably, the numerical result could be obtained by the transient finite element method (LS-Dyna®, version 970).

Although the CACM models have reduced the degree-of-freedoms (DOFs) of the freely-untwisting dsDNA, good agreement is achieved between the numerical simulation and experimental result. Moreover, we would apply the proposed dsDNA CACM model in the analysis of the dsDNA unzipping loading. In the preliminary result of the unzipping dsDNA, the mechanical mechanism of the hydrogen bond failure could be described by the numerical simulation. Furthermore, based on the robust model validated by the experimental results, one would further study the sequence-depended mechanism of the unzipping dsDNA. .

## 2 THEORY

### 2.1 Finite Element Theory

The finite element method considers the minimization of the total potential energy, which includes internal energy, bending energy, twisting energy, the contact energy and the

external energy [8]. Moreover, the complex geometry of the double helix DNA can be described by discrete finite element with few geometrical limitations.

Using the principle of minimum potential energy, one can generate the equations for a constant-strain finite element. For each specific time ( $t = t_i$ ), the total potential energy is a function of the nodal displacements  $X(x, y, z)$  such that  $\pi_p = \pi_p(X)$ . Here the total potential energy is given by

$$\pi_p|_{l=l_0} = (P^{int} + P^{kin} - P^{ext})|_{l=l_0} \quad (1)$$

where  $P^{int}$ ,  $P^{kin}$  and  $P^{ext}$  represent internal energy, kinematical energy and energy of external loading. The above equation can be rewritten as a finite element integrated form [8]. Therefore, the minimal potential energy with respect to each nodal displacement requires that:

$$\begin{aligned} \frac{\partial \pi_p}{\partial \{d\}}|_{l=l_0} &= \left( \iiint_V [\rho][N]^T [N] \{d\} + [B]^T [D] [B] dV \right) \{d\}|_{l=l_0} \\ &- \left[ \{P\} + \iint_S [N_S]^T [T_S] dS \right]|_{l=l_0} = 0 \end{aligned} \quad (2)$$

where  $\{d\}$  represents the nodal vector,  $\{\ddot{d}\}$  represents the nodal acceleration,  $\rho$  represents the density.  $[B]$  is the strain-displacement matrix,  $[D]$  is modulus of elasticity matrix,  $[N]$  is the shape function matrix,  $\{P\}$  is the external load vector and  $[T_S]$  is the traction force matrix. Finally, solving the linear system shown in Eq.(2) at each specific time, one can obtain the  $\{d\}$  and the global nodal vector can be revealed.

## 2.2 Bonding Energies of the dsDNA

In the dsDNA modeling, two kinds of the bonding energies are considered herein. First, we consider the base-stacking interactions, which originate from the weak van der Waals attraction between the polar groups in the adjacent base pairs. Moreover, the hydrogen bond forces between the adjacent base-pairs are considered.

The base stacking energy is a short range interaction, and their total effect could be described by the Lennard-Jones potential from (6-12 potential form [9]). Base-stacking interactions play a significant role in the stabilization of the DNA double helix. By the Crotti-Engesser theorem, one can obtain the L-J potential force versus displacement relationship:

$$f_{LJ} = \frac{12AU_0}{l_0} \left( \frac{h_0 + \Delta l \cos \varphi_0}{h_0 + \Delta l} \right)^3 \left[ 1 - \left( \frac{h_0 + \Delta l \cos \varphi_0}{h_0 + \Delta l} \right)^6 \right] \left[ \frac{h_0(1 - \cos \varphi_0)}{h_0 \tan \varphi_0 (h_0 + \Delta l \cos \varphi_0)} \right] \quad (3)$$

where  $f_{LJ}$  represents the stacking force,  $U_0$  represents the base stacking intensity and  $\Delta l$  represents the distance between the adjacent base pairs.  $l_0$ ,  $h_0$  and  $\varphi_0$  represent the initial specific length, base pair height and folding angle of the dsDNA, respectively [10].

The hydrogen bond (H-bond) force is the interaction between complementary bases. Moreover, the GC base-pair has 3 H-bonds and AT has 2. These bonding energies can transverse all of the bending moments and force, because both the distance ( $R_i$ ) and the angle ( $\theta_{Hb}$ ) between the donor and the acceptor affect the hydrogen bond energy. The single H-bond energy  $E$  of base-pairs could be expressed as [11]:

$$E(R_i, \theta) = \sum_{R_i} AD_0 \left[ 5 \left( \frac{R_0}{R_i} \right)^{12} - 6 \left( \frac{R_0}{R_i} \right)^{10} \right] \cos^4 \theta_{Hb} \quad (4)$$

where  $D_0$  represents the hydrogen bond energies intensity.  $R_0$  and  $R_i$  is the initial and recent distances of the H-bond. Moreover, we assume that the distances of H-bonds are the same along the dsDNA, the B-form DNA have the lowest H-bond potential and D-H-A at same line, and the H atom always at the center of H-bond at initial state. Figure 1 (Fig. 1) illustrates the hydrogen bond model we used, including both GC and AT cases.

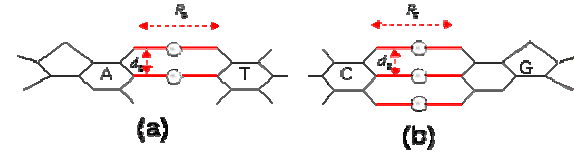


Fig. 1. Schematic illustration of hydrogen model. (a) is the AT hydrogen bond model, and (b) is the GC hydrogen bond model.

Furthermore, we assume that the hydrogen bound model in Fig. 1 would own two degree of freedoms, and the Fig. 2 illustrated the GC-based deformation scheme, and the AT-based deformation behaves similar to the GC one. By the Crotti-Engesser theorem, we could obtain the hydrogen bond reaction axial force by introducing the axial displacement vector  $\Delta r$ :

$$Axial F_{HB}(\Delta r) = \frac{j}{R_0} D_0 \left[ \left( \frac{R_0}{R_0 + \Delta r} \right)^{11} - \left( \frac{R_0}{R_0 + \Delta r} \right)^{13} \right] \quad (5)$$

where  $j = 180$  for GC case and  $j = 120$  for AT case. The two direction shearing reaction forces could be expressed by the shearing displacement  $\Delta y$ :

$$\begin{aligned} s\text{-shear } f_{GC} &= \frac{\partial}{\partial \Delta y} \left\{ E \left( \sqrt{R_0^2 + \Delta y^2} + \frac{d_0 \Delta y}{R_0}, \pi - 2 \frac{\Delta y}{R_0} \right) + E \left( \sqrt{R_0^2 + \Delta y^2}, \pi - 2 \frac{\Delta y}{R_0} \right) \right. \\ &\quad \left. + E \left( \sqrt{R_0^2 + \Delta y^2} - \frac{d_0 \Delta y}{R_0}, \pi - 2 \frac{\Delta y}{R_0} \right) \right\} \\ t\text{-shear } f_{GC} &= 3 \frac{\partial}{\partial \Delta y} E \left( \sqrt{R_0^2 + \Delta y^2}, \pi - 2 \frac{\Delta y}{R_0} \right) \end{aligned} \quad (6)$$

$$s\text{-shear } f_{AT} = \frac{\partial}{\partial \Delta y} \left\{ E \left( \sqrt{R_0^2 + \Delta y^2} + \frac{d_0 \Delta y}{R_0}, \pi - 2 \frac{\Delta y}{R_0} \right) \right. \\ \left. + E \left( \sqrt{R_0^2 + \Delta y^2}, \pi - 2 \frac{\Delta y}{R_0} \right) \right\} \quad (7)$$

$$t\text{-shear } f_{AT} = 2 \frac{\partial}{\partial \Delta y} E \left( \sqrt{R_0^2 + \Delta y^2}, \pi - 2 \frac{\Delta y}{R_0} \right)$$

The two direction bending moment relationships could be expressed by the shearing displacement  $\theta$ :

$$s\text{-bending } M_{GC} = \frac{\partial}{\partial \theta} \{ E(R_1, 2\theta) + E(R_2, 2\theta) + E(R_3, 2\theta) \} \quad (8)$$

$$t\text{-bending } M_{GC} = 3 \frac{\partial}{\partial \theta} E(R_2, 2\theta)$$

$$s\text{-bending } M_{GC} = \frac{\partial}{\partial \theta} \{ E(R_1, 2\theta) + E(R_2, 2\theta) + E(R_3, 2\theta) \} \quad (9)$$

$$t\text{-bending } M_{GC} = 3 \frac{\partial}{\partial \theta} E(R_2, 2\theta)$$

where  $R_1, R_2$  and  $R_3$  equals  $\sqrt{(R_0 + d_0 \theta)^2 + R_0^2 \theta^2}$ ,  $\sqrt{R_0^2 + R_0^2 \theta^2}$  and  $\sqrt{(R_0 - d_0 \theta)^2 + R_0^2 \theta^2}$ . At last, the torque reaction could be expressed as:

$$T_{GC} = 2 \cdot 60 \cdot D_0 (d_{0,GC}^4) \frac{R_0^{10}}{\left[ R_0^2 + d_{0,GC}^2 \theta^2 \right]^7} \theta^3 \cos^4 2 \frac{d_{0,GC}}{R_0} \theta \\ + 8 D_0 \frac{R_0^{11} d_{0,GC} + 6 R_0^9 d_{0,GC}^2 \theta^2}{\left[ R_0^2 + d_{0,GC}^2 \theta^2 \right]^6} \cos^3 2 \frac{d_{0,GC}}{R_0} \theta \sin 2 \frac{d_{0,GC}}{R_0} \theta \quad (10)$$

$$T_{AT} = 2 \cdot 60 \cdot D_{0,AT} (d_0^4) \frac{R_0^{10}}{\left[ R_0^2 + d_{0,AT}^2 \theta^2 \right]^7} \theta^3 \cos^4 2 \frac{d_{0,AT}}{R_0} \theta \\ + 8 D_0 \frac{R_0^{11} d_{0,AT} + 6 R_0^9 d_{0,AT}^2 \theta^2}{\left[ R_0^2 + d_{0,AT}^2 \theta^2 \right]^6} \cos^3 2 \frac{d_{0,AT}}{R_0} \theta \sin 2 \frac{d_{0,AT}}{R_0} \theta \quad (11)$$

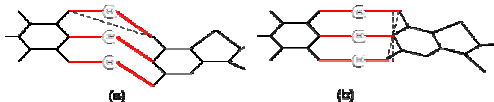


Fig. 2. Schematic illustration of GC-based deformation. (a) is the transverse type deformation and (b) is the rotation type deformation.

### 2.3 dsDNA CACM numerical modeling

In this section, we will construct the CACM model to simulate the dsDNA mechanical behavior. Due to that the classic B-DNA is stable in physiological aqueous solution, its geometrical structure has been chosen as the initial state of the said model, and the Writh number of proposed dsDNA model has been assumed as zero. Moreover, both the major/minor groove and the sequence of the dsDNA were neglected for the sake of simplifying the proposed CACM model. Moreover, the CACM comprises both the clustered atomistic and atomistic-continuum methods.

The numerical modeling of the dsDNA would be divided into two parts. One aspect is the description of the mechanics of the double-helix structure of the nucleotide chain (backbones and base-pairs), where the atoms are bound by the covalent bonds. These atomic groups are

treated as the individual clustered elements by the clustered atomistic mechanics method. However, before constructing the dsDNA numerical model, we must acquire the clustered atomistic properties of the double-helix sugar-phosphate backbone. Therefore, a feasible ssDNA transient finite element model was constructed, based on the continuum beam type elements.

The other aspect lies in the simulation of the binding energies which provide the stability of the dsDNA, such as the van der Waals forces (Eq. 3) between the adjacent base pairs and the hydrogen bonds between the complementary base pairs (Eq. 4-Eq. 11). Therefore, the virtual elements would be established between the clustered elements to represent the binding energies, where the physical properties of the virtual elements could be transferred by the atomistic-continuum method. Fig. 3 indicates concepts of the CACM modeling.

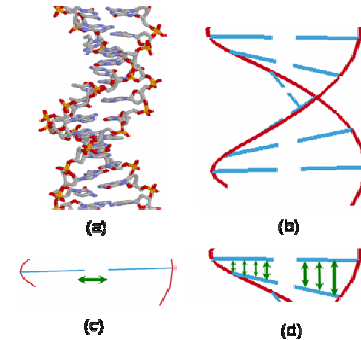


Fig. 3. Schematic illustration of dsDNA CACM model. (a) represents the chemical structure of dsDNA. (b) is the CACM model, including the backbone (red) and base-pairs (blue). The bonding energies are considered in (3) and (4), which are the Hydrogen bond energy and the stacking energies.

This model comprises 147 base pairs, with the initial length of the dsDNA equaling approximately 50nm. In the freely-untwisting dsDNA simulation, one end of the backbone was mechanically fixed. Besides, an external prescribed displacement was applied at the other end, which the prescribed displacement was strictly proportional to the simulation time.

### 3 SIMULATION RESULTS

The dsDNA CACM model consisted of 3,095 clustered elements and 584 virtual elements. The transient finite element model was solved by LS-DYNA3D® with a CPU time of 20,652 seconds on an IBM® SP2 SMP distributed computer.

The simulation results of the reacted forces, sensed by the bottom fixed point versus the external applied displacement, are shown in FIG. 4, where it shows that we achieved good agreement between the numerical and the experimental results. Moreover, the finite element simulation results of stretching the freely-untwisting dsDNA revealed a continuously structural transition, which

may be characterized as three main stages in the stretching process [12].

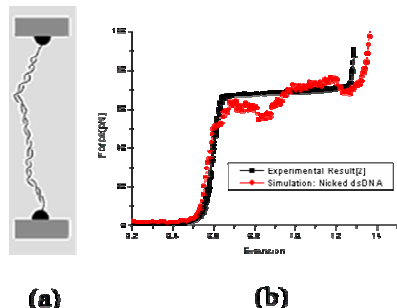


Fig. 4. The dsDNA clustered atomistic-continuum model (CACM) and simulation result. (a) is the schematic illustration of the nicked dsDNA boundary conditions. (b) is the simulation result based on the CACM, where the plateau is occurred at about 65 pN at experimental[2] and simulation results (on average).

Based on the validated dsDNA CACM model, the unzipping loading is applied on the model to simulate the dsDNA unzip mechanics. One strand of the dsDNA end is fixed and the other strand is applied to a prescribed motion. The simulation result is shown in Fig. 5. The reaction force plot in Fig. 6 indicated that the saw-tooth pattern of the hydrogen bond opening, and the a plateau would occur due to the rotation of the backbone, where no hydrogen bond breaks.

#### 4 CONCLUSION

In this paper, a novel clustered atomistic-continuum method, based on a transient finite element method was proposed to simulate the dsDNA mechanics. To completely consider the hydrogen bond effects between base pairs, the detail theoretical derivation would be emphasized. Good agreement was achieved between the numerical simulation and experimental results in both freely-untwisting dsDNA. Furthermore, based on this robust model, the mechanics of the dsDNA unzipping could be studied.

#### ACKNOWLEDGEMENT

We are grateful to Dr. J. Marko, Dr. S. B. Smith and Dr. C. Bustamante. Also, we thank Dr. A. Sarkar for valuable discussions on single molecular experiment. C. A. thanks Dr. J. Day and Dr. C. Tsay for discussions on numerical simulation technique.

#### REFERENCES

- [1] C. Bustamante, Z. Bryant and S. B. Smith, "Ten years of tension: single-molecule DNA mechanics," *Nature*, 421, 423-427, 2003.
- [2] J. F. Leger, G. Romans, A. Sarkar, J. Robert, L. Bourdieu, D. Chatenay and J. F. Marko, "Structural transitions of a twisted and stretched DNA module," *Phys. Rev. Letters*, 83, 1066-1069, 1999.
- [3] A. Sarkar, J. F. Leger, D. Charenay and J. F. Marko, "Structural transitions in DNA driven by external force and torque", *Phys. Rev. E.*, 63, 51903, 2001

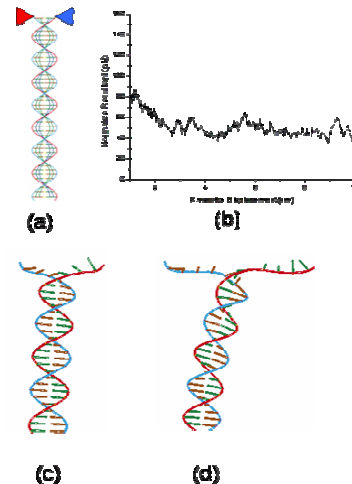


Fig. 5. The dsDNA unzip simulation via CACM. (a) is the schematic illustration of the unzip dsDNA boundary conditions, where red triangle means the fixed end and the blue one is applied a prescribed motion (b) is the reaction forces sensed by the fixed point. (c) and (d) is the continuous deformation of unzipping dsDNA.

- [4] C. G. Baumann, V. A. Bloomfield, S. B. Smith, C. Bustamante and M. D. Wang, "Stretching of single collapsed DNA molecules", *Biophys. J.*, 78, 1965-1978, 2000.
- [5] C. Benham, "Onset of writhing in circular elastic polymers," *Phys. Rev. A*, 39, 2582-2586, 1989.
- [6] J. F. Marko and E. D. Siggia, "Statistical mechanics of supercoiled DNA," *Phys. Rev. E*, 52, 2912-2938, 1995.
- [7] H. Zhou, Y. Zhang and Z. Ou-Yang, "Elastic property of single double stranded DNA molecules: theoretical study and comparison with experiments," *Phys. Rev. E*, 62, 1045-1058, 2000.
- [8] R. D. Cook, D. S. Malkus and M. E. Plesha, "Concepts and Application of Finite Element Analysis", Wiley, 367-428, 1989.
- [9] W. Saenger, "Principles of Nucleic Acid Structure," Springer-Verlag, 1984
- [10] C. A. Yuan and K. N. Chiang, "Investigation of dsDNA stretching meso-mechanics using finite Element Method", 2004 Nanotechnology Conference, March 7-11, 2004, Boston, Massachusetts, U.S.A.
- [11] G. A. Jeffery, W. Saenger, "Hydrogen Bonding in Biological Structures", 1st ed., Springer-Verlag, Germany, 1994
- [12] C. A. Yuan, C. N. Han and K. N. Chiang, "Atomistic to Continuum Mechanical Investigation of ssDNA and dsDNA using Transient Finite Element Method," Inter-Pacific Workshop on Nanoscience and Nanotechnology, Nov. 22-Nov. 24, 2004, City University of Hong Kong, Hong Kong SAR